⌘ *Author's Choice*

THE JOURNAL OF BIOLOGICAL CHEMISTRY VOL. 286, NO. 42, pp. 37023–37031, October 21, 2011

Increased Bone Mass in Mice after Single Injection of Anti-receptor Activator of Nuclear Factor-κB Ligand-neutralizing Antibody

EVIDENCE FOR BONE ANABOLIC EFFECT OF PARATHYROID HORMONE IN MICE WITH FEW OSTEOCLASTS[*] [S]

Received for publication, April 7, 2011, and in revised form, August 15, 2011 Published, JBC Papers in Press, August 23, 2011, DOI 10.1074/jbc.M111.246280

Yuriko Furuya[‡], Kaoru Mori[‡], Tadashi Ninomiya[§], Yoshiya Tomimori[‡], Sakae Tanaka[¶], Naoyuki Takahashi[§], Nobuyuki Udagawa[§‖], Kohji Uchida[‡], and Hisataka Yasuda[1]**

*From the [‡]Nagahama Institute for Biochemical Science, Nagahama Branch, Oriental Yeast Co., Limited, 50 Kano-cho Nagahama, Shiga 526-0804, the **Bioindustry Division, Oriental Yeast Co., Limited, 3-610 Azusawa, Itabashi-ku, Tokyo 174-8505, the [§]Institute for Oral Science and [‖]Department of Biochemistry, Matsumoto Dental University, 1780 Gobara, Hiro-oka, Shiojiri, Nagano 399-0781, and the [¶]Department of Orthopaedic Surgery, Faculty of Medicine, University of Tokyo, 7-3-1 Hongo, Bunkyo-ku, Tokyo 113-0033, Japan*

Background: Receptor activator of nuclear factor-κB ligand is a pivotal osteoclast differentiation factor.
Results: Daily injection of parathyroid hormone increased bone mass by stimulating bone formation in the anti-receptor activator of nuclear factor-κB ligand antibody-treated mice.
Conclusion: Parathyroid hormone exerted its bone anabolic activity in mice with few osteoclasts.
Significance: Parathyroid hormone requires no osteoclasts for stimulating bone formation.

Receptor activator of nuclear factor-κB ligand (RANKL) is a pivotal osteoclast differentiation factor. To investigate the effect of RANKL inhibition in normal mice, we prepared an anti-mouse RANKL-neutralizing monoclonal antibody (Mab, clone OYC1) and established a new mouse model with high bone mass induced by administration of OYC1. A single subcutaneous injection of 5 mg/kg OYC1 in normal mice significantly augmented the bone mineral density in the distal femoral metaphysis from day 2 to day 28. The OYC1 treatment markedly reduced the serum level of tartrate-resistant acid phosphatase-5b (TRAP-5b, a marker for osteoclasts) on day 1, and this level was undetectable from day 3 to day 28. The serum level of alkaline phosphatase (a marker for osteoblasts) declined significantly following the reduction of TRAP-5b. Histological analysis revealed few osteoclasts in femurs of the treated mice on day 4, and both osteoclasts and osteoblasts were markedly diminished on day 14. Daily injection of parathyroid hormone for 2 weeks increased the bone mineral density in trabecular and cortical bone by stimulating bone formation in the OYC1-treated mice. These results suggest that parathyroid hormone exerted its bone anabolic activity in mice with few osteoclasts. The mouse anti-RANKL neutralizing antibody OYC1 may be a useful tool to investigate unknown functions of RANKL *in vivo*.

Receptor activator of nuclear factor-κB ligand (RANKL)[2] is a member of the tumor necrosis factor (TNF) superfamily that binds to its receptor RANK, which is expressed on osteoclasts and their progenitors (1, 2). The interaction of RANK with RANKL is required for osteoclast formation, differentiation, activation, and survival (3, 4). Osteoprotegerin (OPG) is a natural decoy receptor for RANKL (5–7). Bone resorption is mediated by RANKL-RANK signaling, and excessive osteoclastic bone resorption plays a central role in the pathogenesis of age-related bone loss and microstructural deterioration, leading to fragility fractures (8–10).

In addition to regulation of bone homeostasis, RANKL also plays an important role in the immune system, cancer metastasis, and differentiation of mammary gland stem cells (11–17). These studies suggest that RANKL may have further unknown functions *in vivo*. To investigate these possible functions, OPG and soluble RANK (sRANK) have been used in previous studies (4–7, 18–20). However, pharmacokinetic studies have shown that these recombinant proteins are not maintained in serum for a long period, which makes it necessary to inject the proteins

[*] H. Y. is an employee of Oriental Yeast Co., Limited.
[S] The on-line version of this article (available at http://www.jbc.org) contains supplemental Methods and Fig. 1.
⌘ *Author's Choice*—Final version full access.
[1] To whom correspondence should be addressed. Tel.: 81-3-3968-1192; Fax: 81-3-3968-4863; E-mail: hyasuda@oyc.co.jp.

[2] The abbreviations used are: RANKL, receptor activator of nuclear factor-κB ligand; ALP, alkaline phosphatase; BFR/BS, bone formation rate/bone surface; BMD, bone mineral density; BV/TV, bone volume/tissue volume; ES/BS, eroded surface/bone surface; hRANKL, human soluble RANKL; huRANKL mice, human RANKL knock-in mice; Mab, monoclonal antibody; MAR, mineral apposition rate; mRANKL, mouse soluble RANKL; N.Ob/BS, osteoblast number/bone surface; N.Oc/BS, osteoclast number/bone surface; Ob.S/BS, osteoblast surface/bone surface; Oc.S/BS, osteoclast surface/bone surface; OPG, osteoprotegerin; pNPP, *p*-nitrophenyl phosphate; pQCT, peripheral quantitative computed tomography; PTH, parathyroid hormone; sRANK, soluble RANK; sRANKL, soluble RANKL; SXA, single-energy x-ray absorptiometry; Tb.Th, trabecular bone thickness; TNF, tumor necrosis factor; TRAIL, TNF-related apoptosis-inducing ligand; TRAP, tartrate resistant acid phosphatase; X-SSI, *x* axis strength strain index; ANOVA, analysis of variance.

into animals frequently, *e.g.* every day to inhibit RANKL *in vivo*. OPG also binds to the TNF-related apoptosis-inducing ligand (TRAIL) and inhibits TRAIL functions (21, 22), although the affinity of sRANK for soluble RANKL (sRANKL) is lower than that of OPG (3, 4, 23). Therefore, OPG and sRANK may not be suitable for specific inhibition of RANKL *in vivo*.

Denosumab, a fully human anti-RANKL-neutralizing monoclonal antibody (Mab), has recently been approved in Europe and the United States for treatment of osteoporosis and in the United States for prevention of skeletal related events in patients with bone metastases from solid tumors. Because denosumab is not cross-reactive with rodent RANKL, its evaluation in preclinical studies was performed in cynomolgus monkeys or human RANKL knock-in mice (huRANKL mice), in which exon 5 in mouse *rankl* was replaced with that in human *RANKL* (24). However, there were several abnormalities in huRANKL mice, including a decreased osteoclast number, increased trabecular bone mineral density (BMD), and a reduced osteoblast surface, compared with normal mice, and these abnormalities reduce the suitability of these mice for analysis of RANKL inhibition with an anti-RANKL-neutralizing Mab such as denosumab (24–27).

Parathyroid hormone (PTH) is the only bone anabolic agent that is currently used for treatment of osteoporosis in humans. The precise mechanisms through which PTH increases bone formation *in vivo* are unknown, but previous studies have shown that osteoclasts are required for the bone anabolic effect of PTH (27, 28). To investigate the effects of RANKL inhibition on bone mass and other features in normal mice, we prepared an anti-mouse RANKL-neutralizing Mab (OYC1) and established a novel mouse osteopetrotic model with high bone mass induced by administration of OYC1 to normal mice. In this study, we characterized OYC1 and established a method for long term neutralization of RANKL *in vivo* in normal mice, in which a single injection of OYC1 neutralized RANKL activity for 4 weeks. We examined the effect of OYC1 on bone mass and showed the utility of OYC1 for evaluating the bone anabolic effect of PTH.

EXPERIMENTAL PROCEDURES

Reagents—Two hybridoma-producing mouse RANKL Mabs (clones OYC1 and OYC2) were subcloned from hybridoma kindly provided by Dr. Okumura (Juntendo University School of Medicine) and manufactured by Oriental Yeast Co. (29). Recombinant human OPG-Fc and mouse soluble RANKL (sRANKL) were purchased from R&D Systems. PTH(1–34) and calcein were purchased from Sigma. Other reagents were purchased from Nacalai Tesque, Inc. (Japan).

Bone Analysis in Mice Treated with mRANKL Mab (OYC1) in Vivo—Five-week-old female C57BL/6N mice were purchased from Charles River Inc. and acclimated for 1 week under standard laboratory conditions at 24 ± 2 °C and 40–70% humidity. Mice were treated according to the institutional ethical guidelines for animal experimentation and safety.

To establish the effect of the mRANKL Mabs on bone mass, the neutralizing antibody (OYC1) and non-neutralizing control antibody (OYC2) were administered intraperitoneally to 6-week-old female mice ($n = 5$) three times per week for 2 weeks. Calcein was injected twice subcutaneously for labeling on days 10 and 13. At 12 h after the last administration, femurs were extirpated and fixed with 70% ethanol.

To determine the suboptimal dose of OYC1 for increasing the BMD, various doses (0.5, 1, 1.5, 5, and 15 mg/kg) of OYC1 or vehicle (PBS) were injected subcutaneously in 6-week-old female mice ($n = 5$) once on day 0. Blood samples and both femurs were obtained on day 14, and the femurs were fixed with 70% ethanol.

To examine the time course of the effect of OYC1, 5 mg/kg OYC1 or PBS was administered subcutaneously to 6-week-old female mice ($n = 5–6$) on day 0. The mice were sacrificed on days 4, 7, 14, and 28, and sera and femurs were obtained on these days. To examine the early part of the time course in more detail, 5 mg/kg OYC1 or PBS was administered subcutaneously to 6-week-old female mice ($n = 5–6$) on day 0. The mice were sacrificed on days 1–4, and sera and femurs were obtained on these days.

To examine the utility of the RANKL-neutralizing model, we tested whether PTH could induce bone formation in OYC1-treated mice. OYC1 (5 mg/kg) or PBS was injected once in 6-week-old female mice ($n = 5$). After 4 days, PTH (160 μg/kg) or PBS was injected subcutaneously daily for 2 weeks in these mice. The mice treated with PTH after transient neutralization of RANKL with OYC1 were sacrificed on day 18, and sera, femurs, and tibias were collected.

Measurement of BMD—BMDs were determined in fixed right femurs by single energy x-ray absorptiometry (SXA, DCS-600EX; Aloka, Japan). The femurs were divided into 20 equal regions from distal (region 1) to proximal (region 20), and the BMD of each region was measured by SXA. In some experiments, BMD was measured by peripheral quantitative computed tomography (pQCT, XCT Research SA+, Stratec Medizintechnic, Pforzheim, Germany) using a voxel size of 0.08 × 0.08 × 0.46 mm. Image analysis was carried out using integrated XCT 2000 software version 6.00f. Total BMD at 0.8 or 1.0 mm from the growth plate is shown due to the marked increase of BMD after injection of OYC1. Cortical bone was defined based on BMD >690 mg/cm^3 at the femoral metaphysis. Cortical area (mm^2), cortical thickness (mm), periosteal perimeter of the cortical bone (in mm), endosteal perimeter of the cortical bone (in mm), *x* axis strength-strain index (in mm^3), *y* axis strength-strain index (in mm^3), and polar strength-strain index (in mm^3) were measured. Three-dimensional digital images of femurs were reconstructed by micro-CT analysis at 0.2–1.2 mm from the growth plate using a ScanXmate-A080 (Comscan Tecno). Analysis of micro-CT images was performed with TRI/3D-Bon (Ratoc System Engineering Co., Japan).

Histomorphometry—Fixed and undecalcified femurs were embedded in glycol methacrylate or methyl methacrylate and 3–5-μm sections in the proximal region and distal femoral metaphysis of each femur were cut longitudinally and stained with toluidine blue O. Some samples were stained by the Villanueva method. Histomorphometry was performed with an image analysis system (Ostoplan II, Carl Zeiss, New York) linked to a light microscope. Histomorphometric measurements were made at ×400 magnification in the secondary

spongiosa area. The bone volume/tissue volume (BV/TV, %), trabecular bone thickness (Tb.Th, μm) osteoclast surface/bone surface (Oc.S/BS, %), eroded surface/bone surface (ES/BS, %), osteoclast number/bone surface (N.Oc/BS, 1/mm), osteoblast surface/bone surface (Ob.S/BS, %), osteoblast number/bone surface (N.Ob/BS, 1/mm), the mineral apposition rate (MAR, μm/day), bone formation rate/bone surface (BFR/BS, mm^3/mm^2/year) were calculated and expressed according to standard formulas and nomenclature (30). For TRAP staining, 3-μm sections in the proximal metaphysis of the undecalcified tibia were cut longitudinally and stained with TRAP.

Measurement of Biomarkers and OYC1 in Serum—Serum levels of calcium and ALP were measured according to the manufacturers' instructions using a calcium C assay and a LabAssay ALP (Wako, Japan) (*p*-nitrophenyl phosphate (pNPP) assay), respectively. Serum mouse osteocalcin, TRAP-5b, and intact PTH were measured by enzyme-linked immunosorbent assay (ELISA) according to manufacturers' instructions (Biomedical Technologies, MA; Immunodiagnostic Systems, AZ; and Immutopics, CA; respectively).

The serum level of OYC1 was measured by ELISA. Recombinant mRANKL was coated on an ELISA plate (Nunc) at 2.5 nM, and the serum antibody titer was detected by HRP-conjugated rat IgG2a (Zymed Laboratories Inc.). Each value was determined by absorbance at 450 nm using a microplate reader.

Statistical Analysis—Results are expressed as means ± S.D. for all data. Significance of differences was determined by ANOVA with a Dunnett's test or Student's *t* test. $p < 0.05$ was considered significant.

RESULTS

Effect of Mouse RANKL Mabs (OYC1 and OYC2) in Vitro and in Vivo—To characterize the anti-mRANKL Mabs, OYC1 and OYC2, a binding assay was performed by direct ELISA. Both antibodies recognized recombinant mouse sRANKL (mRANKL), including the extracellular domain from Arg-72 to Asp-316 (supplemental Fig. 1*A*). Neither OYC1 nor OYC2 bound to mouse TRAIL (data not shown). OYC1 neutralized mRANKL-induced osteoclastogenesis in a dose-dependent manner. OYC1 (0.2 μg/ml) and human OPG-Fc (0.1 μg/ml) completely suppressed osteoclast formation induced by 5 nM mRANKL, but OYC2 did not do so (supplemental Fig. 1*B*). OYC1 did not bind to or inhibit human sRANKL (hRANKL, supplemental Fig. 1*B*, and data not shown). Morphological examination of cells cultured in the presence of mRANKL with or without OYC1 confirmed the complete inhibition of formation of TRAP-positive multinucleated cells (supplemental Fig. 1*C*). These results indicate that OYC1 is a neutralizing Mab and OYC2 is a non-neutralizing Mab.

To investigate the effect of the Mabs *in vivo*, 15 mg/kg OYC1 or OYC2 or vehicle (PBS) were administered intraperitoneally to mice three times per week for 2 weeks (Fig. 1*A*). OYC2 showed no effect on BMD in femurs of the treated mice, whereas OYC1 markedly increased the BMD, especially in the distal metaphysis, compared with OYC2 and vehicle. In contrast, OYC1 had little effect on BMD in the femoral diaphysis (Fig. 1*A*). Photomicrographs of toluidine blue O staining of femurs of the OYC1-treated mice also indicated a marked

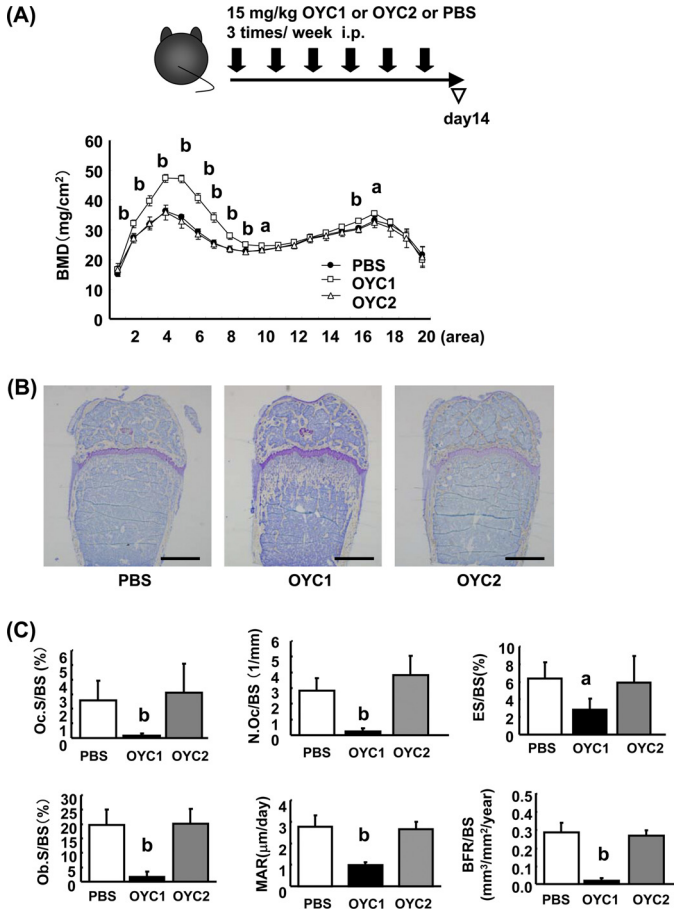

FIGURE 1. **Effects of mRANKL monoclonal antibody OYC1 on BMD, bone structure, and bone histomorphometry in mice.** Female 6-week-old C57BL/6N mice ($n = 5–6$) were injected intraperitoneally (*i.p.*) with 15 mg/kg anti-mouse RANKL Mab OYC1 or OYC2 or PBS three times per week for 2 weeks. At 12 h after the last administration, femurs were extirpated and fixed with 70% ethanol. *A,* right femur was partitioned into 20 areas, and BMD of each part was measured by SXA. *B,* toluidine blue staining of the distal femoral metaphysis. *C,* histomorphometry was performed on undecalcified sections. Oc.S/BS, N.Oc/BS, ES/BS, Ob.S/BS, MAR. and BFR/BS were measured. *Bar,* 1 mm. Data are shown as the mean ± S.D. *a*, $p < 0.05$; *b*, $p < 0.01$ (ANOVA) *versus* PBS.

increase in bone mass in the distal femoral metaphysis (Fig. 1*B*). Histomorphometry revealed marked decreases in Oc.S/BS, N.Oc/BS, and ES/BS (Fig. 1*C*) and also marked decreases in Ob.S/BS, MAR, and BFR/BS in the secondary trabecular area in femurs in OYC1-treated mice (Fig. 1*C*). Because OYC2 exhibited no effect on bone mass (Fig. 1, *A–C*), we used vehicle (PBS) as a negative control in the following experiments.

Optimization of Single Dose of OYC1 for Increasing Bone Mass in Mice—To establish a simple method for increasing bone mass, various doses (0.5, 1, 1.5, 5, and 15 mg/kg) of OYC1 were injected subcutaneously once in female mice, and femurs and sera were obtained for analysis after 2 weeks. SXA and pQCT analyses showed that the total BMD in the femurs was augmented significantly at doses of 5 and 15 mg/kg OYC1 (Fig. 2*A* and data not shown). Micro-CT analysis of the femurs confirmed marked augmentation of bone mass at 5 and 15 mg/kg OYC1 (Fig. 2*B*). Histomorphometric analysis of the distal femoral metaphysis in mice given 5 and 15 mg/kg OYC1 also showed significant decreases in Ob.S/BS, Oc.S/BS, N.Oc/BS, and ES/BS (Fig. 2*C*). Consistent with these results, serum

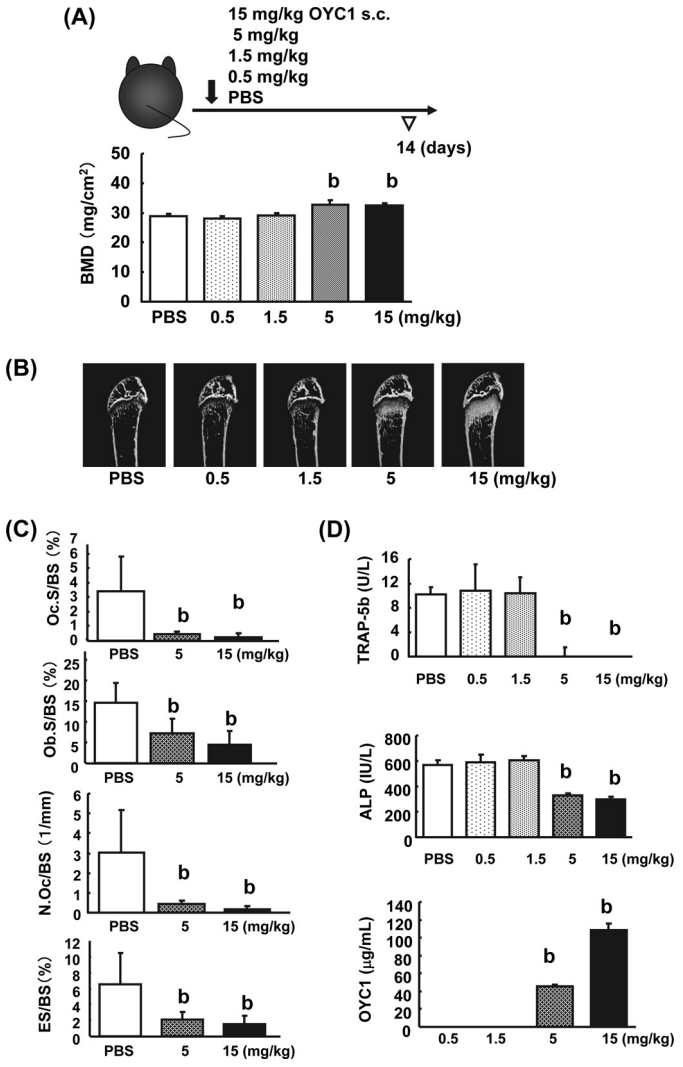

FIGURE 2. **Suboptimal dose of OYC1 required to increase bone mass.** Various doses (0.5, 1, 1.5, 5, and 15 mg/kg) of OYC1 or PBS were injected subcutaneously (*s.c.*) in 6-week-old female mice once ($n = 5$). After 2 weeks, blood samples and femurs were collected, and the femurs were fixed with 70% ethanol. *A,* femoral trabecular bone mass was measured by SXA analysis. *B,* bone structure in the trabecular area was analyzed by micro-CT. *C,* femoral trabecular bone was measured by histomorphometry. Ob.S/BS, Oc.S/BS, N.Oc/BS, and ES/BS were measured in the PBS and OYC1 (5 and 15 mg/kg) groups. *D,* serum TRAP-5b, ALP, and OYC1 levels were measured by ELISA or pNPP assay. Data are shown as the mean ± S.D. *b*, $p < 0.01$ (ANOVA) *versus* PBS.

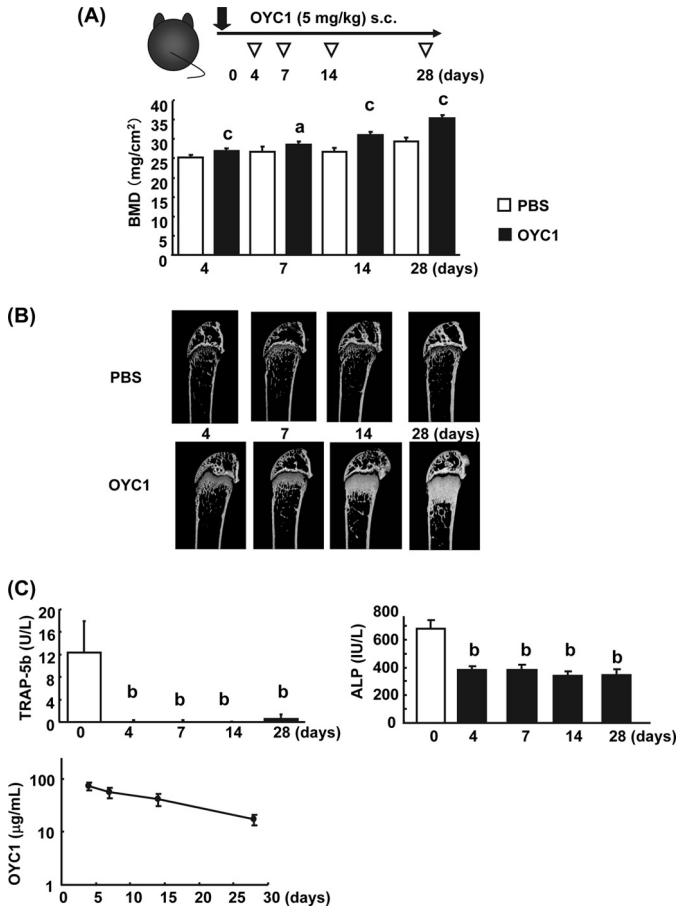

FIGURE 3. **Time course of the effect of OYC1 on bone mass (days 4 to 28).** *A,* OYC1 (5 mg/kg) was administered subcutaneously (*s.c.*) to 6-week-old female mice ($n = 5$–6) on day 0. The mice were sacrificed on days 4, 7, 14, and 28. Total BMD in femurs was measured by SXA analysis. *B,* bone structure in the trabecular area was analyzed by micro-CT. *C,* serum TRAP-5b, ALP, and OYC1 levels were measured by ELISA or pNPP assay. Data are shown as the mean ± S.D. *a*, $p < 0.05$; *c*, $p < 0.001$ *versus* PBS (Student's *t* test); *b*, $p < 0.01$ (ANOVA) *versus* value on day 0.

TRAP-5b and ALP decreased to similar levels at 5 and 15 mg/kg OYC1 (Fig. 2*D*). There was no difference in the serum calcium concentration at any dose of OYC1 (data not shown). Pharmacokinetic studies showed rapid clearance of OYC1 at doses of 0.5 and 1.5 mg/kg but significantly higher serum concentrations of OYC1 of >40 and >100 μg/ml at 5 and 15 mg/kg, respectively (Fig. 2*D*).

Denosumab has been characterized as a drug with long term efficacy in clinical trials (31). The concentration of denosumab in serum remained high for a week after injection in hRANKL knock-in mice (24). To examine the duration of efficacy of OYC1, we examined the time course of the effects of OYC1 in mice by measuring total BMD, and the concentrations of serum TRAP-5b, ALP, and OYC1 between days 4 and 28 (Fig. 3, *A*–*C*). OYC1 significantly elevated femoral total BMD in a time-dependent manner from days 4 to 28 after a single subcutaneous injection (Fig. 3*A*). Expansion of the dense bone structure in the trabecular area was accompanied by augmentation of total BMD, which was sustained until day 28 (Fig. 3, *A* and *B*). Surprisingly, the concentrations of OYC1 remained at >50 μg/ml in serum until day 14 and at >10 μg/ml until day 28 (Fig. 3*C*). Maintenance of the high OYC1 concentration resulted in a continued increase in bone mass daily until day 28 (Fig. 3, *A* and *B*). To confirm this long term effect of OYC1, biomarkers of bone turnover were examined. OYC1 markedly decreased serum TRAP-5b and ALP levels on day 4, and these levels then remained constant until day 28 (Fig. 3*C*). Interestingly, the TRAP-5b level in the OYC1-treated mice was almost undetectable between days 4 and 28 (Fig. 3*C*). In contrast, the ALP level in the treated mice was reduced to half the level of the vehicle between days 4 and 28 (Fig. 3*C*).

To examine the time course of the effects of OYC1 in more detail in the early period, sera and femurs were collected on days 1–4. Analyses showed that OYC1 significantly increased total BMD in the trabecular area on day 2 and then increased BMD in a time-dependent manner, consistent with micro-CT imaging data (Fig. 4*B*). Surprisingly, a marked decrease of

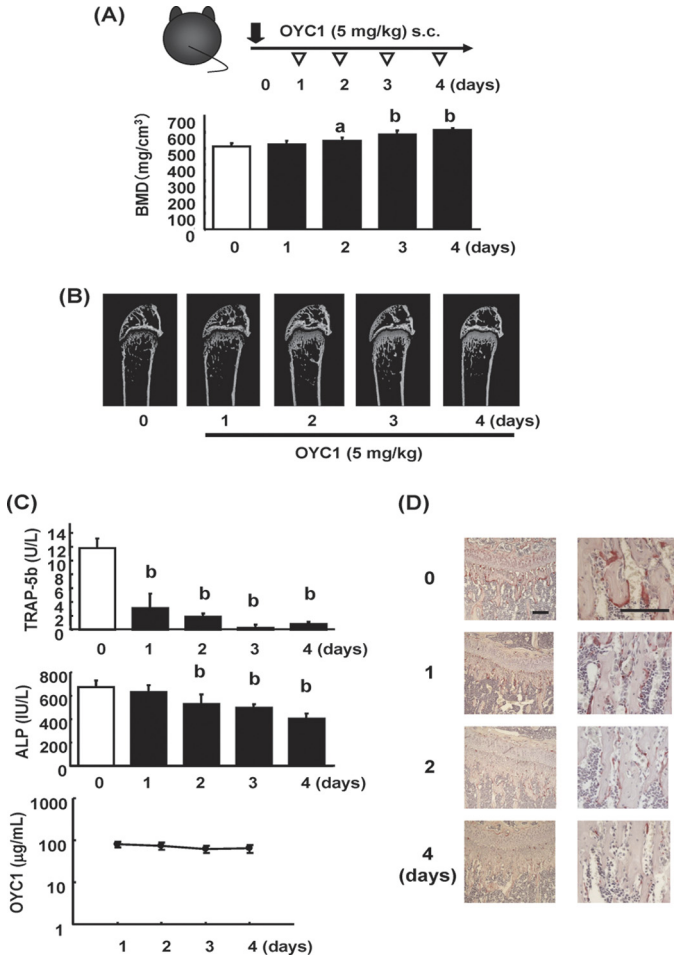

FIGURE 4. **Time course of the effect of OYC1 on bone mass (days 1 to 4).** *A,* OYC1 (5 mg/kg) was administered subcutaneously to 6-week-old female mice ($n = 5–6$) on day 0, and mice were sacrificed on days 1–4. Total BMD was measured by pQCT at 1.0 mm from the distal femoral growth plate. *B,* bone structure in the trabecular area was analyzed by micro-CT. *C,* serum TRAP-5b, ALP, and OYC1 levels were measured by ELISA or pNPP assay. *D,* TRAP staining of undecalcified sections of tibia in OYC1-treated mice are shown on the *left* (*bar,* 100 μm). and high power fields are shown on the *right* (*bar,* 100 μm). Data are shown as the mean ± S.D. *a,* $p < 0.05$; *b,* $p < 0.01$ (ANOVA) *versus* value on day 0.

serum TRAP-5b was observed on day 1, with no change in ALP apparent on day 1 (Fig. 4*C*). The significant decrease of ALP following that of TRAP-5b indicated down-regulation of bone turnover. Concentrations of OYC1 in serum declined from day 1 to day 4 but were still >90 μg/ml on day 4 (Fig. 4*C*). To investigate whether the serum TRAP-5b level reflected the conditions of osteoclasts, histological sections of the trabecular bone in tibia of the OYC1-treated mice were stained for TRAP (Fig. 4*D*). Consistent with the decrease in serum TRAP-5b, there were less TRAP-positive cells (osteoclasts) in the trabecular bone in the OYC1-treated mice on day 1, and only a few osteoclasts were observed in the trabecular bone on day 4.

Anabolic Effect of PTH on Trabecular and Cortical Bones in OYC1-treated Mice—Optimization of the dose and time course effects of OYC1 was performed with the goal of establishing a method for making an osteoclast-depleted mouse model. The above results indicate that single administration of 5 mg/kg OYC1 is suitable for depletion of osteoclasts from days 4 to 28. To examine the bone anabolic effect of PTH in the osteoclast-depleted mice, PTH was injected daily for 2 weeks into mice that had been treated with OYC1 for 4 days. pQCT analysis revealed that administration of PTH and OYC1 increased the total BMD in trabecular bone independently and synergistically (PBS, 465 ± 24; PTH, 607 ± 8; OYC1, 634 ± 40; PTH + OYC1, 719 ± 14 mg/cm^3) (Fig. 5*A*). In contrast, the total BMD in cortical bone was augmented in the PTH groups (PTH and PTH + OYC1) but not with OYC1 treatment alone (PBS, 981 ± 7; PTH, 1001 ± 7; OYC1, 978 ± 17; PTH + OYC1, 1013 ± 15 mg/cm^3) (Fig. 5*B*). The robust depletion of osteoclasts did not affect the anabolic effect of PTH on trabecular and cortical bones. PTH and OYC1 also tended to increase the cortical area, cortical thickness, and polar-SSI, indicating a synergistic effect on bone strength (Table 1). Micro-CT images confirmed the marked increases in trabecular bone mass in mice treated with PTH or OYC1 alone and the synergistic increase with treatment with PTH + OYC1 (Fig. 5*C*).

To investigate the mechanisms by which PTH increased bone mass in OYC1-treated mice, bone histomorphometrical analysis was carried out (Table 2). Administration of PTH or OYC1 significantly increased BV/TV and Tb.Th. PTH alone significantly increased osteoblast parameters such as N.Ob/BS, Ob.S/BS, MAR, and BFR/BS. In contrast, OYC1 alone significantly decreased osteoclast parameters such as N.Oc/BS, Oc.S/BS, and ES/BS to almost zero with significant reduction of osteoblast parameters such as N.Ob/BS, Ob.S/BS, MAR, and BFR/BS. Administration of PTH to OYC1-treated mice significantly augmented Tb.Th, N.Ob/BS, Ob.S/BS, MAR, and BFR/BS compared with OYC1-treated mice. PTH treatment did not change any osteoclast parameters in normal and OYC1-treated mice. Only ES/BS was slightly reduced by PTH treatment in normal mice.

Histological analysis showed that labeled thickness increased in the PTH-treated groups (PTH *versus* PBS; PTH + OYC1 *versus* OYC1). Histological analysis also revealed that osteoblasts in the PTH-treated groups (PTH and PTH + OYC1) showed mature cuboidal morphology, but the cells in the PTH-untreated groups (PBS and OYC1) did inactivate flat morphology (Fig. 5*D*). PTH treatment also changed the morphology and size of osteocytes and bone lacuna in normal and OYC1-treated mice. In addition, polarization microscopy confirmed that PTH stimulated new bone formation (Fig. 5*D*). Although PTH activated osteoclasts in normal mice, pretreatment of the mice with OYC1 depleted osteoclasts almost perfectly even after the PTH treatment (Table 2 and Fig. 5*D*).

To confirm the anabolic effect of PTH in OYC1-treated mice, biomarkers of bone turnover were examined (Fig. 5*E*). As shown in Fig. 3*C*, OYC1 markedly reduced serum TRAP-5b and ALP levels but did not change osteocalcin level. In contrast, PTH significantly increased TRAP-5b and osteocalcin levels but showed no effect on ALP level. Administration of PTH to OYC1-treated mice increased osteocalcin level without affecting TRAP-5b and ALP levels. OYC1 treatment inhibited the PTH-induced elevation in TRAP-5b and reduced the level to almost zero, comparable with treatment with OYC1 alone. Serum intact PTH level was measured to investigate the possible mechanisms of PTH and/or OYC1 treatment. OYC1 slightly reduced intact PTH level, but PTH showed no effect.

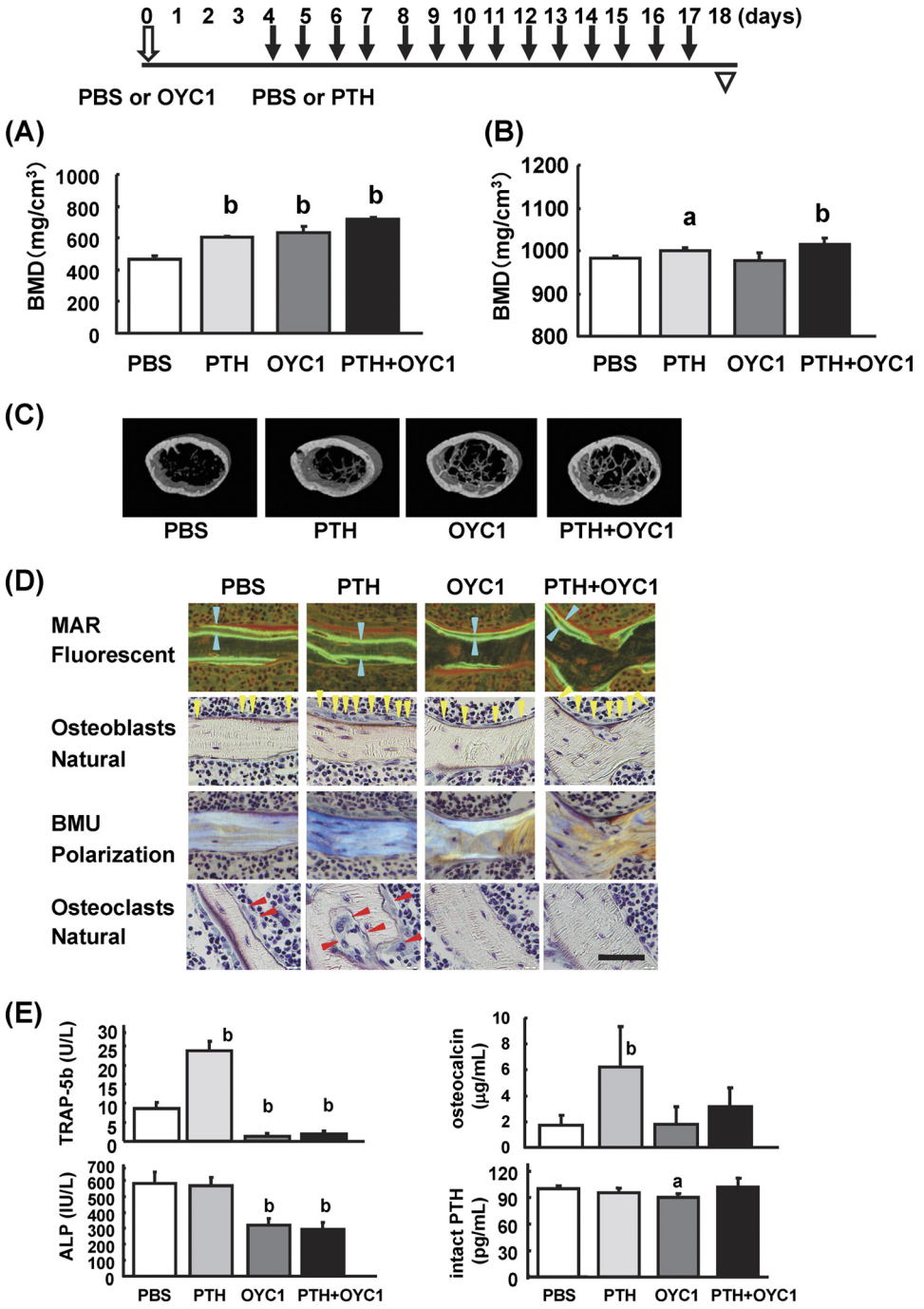

FIGURE 5. **Evaluation of PTH in osteoclast-depleted mice pretreated with OYC1.** OYC1 (5 mg/kg) or PBS was administered subcutaneously to 6-week-old female mice ($n = 5$) on day 0 and PTH (160 μg/kg) or PBS was injected subcutaneously daily from days 4 to 17. Femurs and sera were obtained on day 18. *A,* total BMD was measured by pQCT at 0.8 mm from the distal femoral growth plate. *B,* cortical BMD in the femoral diaphysis was measured by pQCT. *C,* bone structure in the secondary trabecular area was analyzed by micro-CT. *D,* histological data were obtained under fluorescent light, natural light, and polarization using undecalcified sections of each group. Each *arrowhead* indicated labeled thickness (*blue*); osteoblasts (*yellow*); and osteoclasts (*red*). *MAR,* mineral apposition rate; *BMU,* basic multicellular unit. *Bar,* 50 μm. *E,* serum TRAP-5b, osteocalcin, and intact PTH were measured by ELISA. Serum ALP was measured by pNPP assay. Data are shown as the mean ± S.D. *a*, $p < 0.05$; *b*, $p < 0.01$ (ANOVA) *versus* PBS.

DISCUSSION

In this study, we established a method for rapid depletion of osteoclasts in mice by strong inhibition of RANKL activities with a single subcutaneous injection of an anti-mouse RANKL-neutralizing Mab, OYC1. There are several important characteristics of OYC1 that induce osteopetrotic high bone mass in mice. First, OYC1 is specific to mouse RANKL, because it binds to and neutralizes mRANKL but not hRANKL and TRAIL, which are recognized by OPG. Thus, the effects of RANKL inhibition by OYC1 and the therapeutic effects of denosumab can be studied in normal mice. This avoids using huRANKL mice, which have abnormalities such as decreased osteoclasts and increased trabecular bone mass compared with normal mice (24–27). OYC1 may also be useful for investigation of the effect

TABLE 1

Effects of PTH, OYC1, and PTH + OYC1 on cortical bone indices in treated mice

The following abbreviations are used: PERI, periosteal perimeter of the cortical bone; ENDO, endosteal perimeter of the cortical bone; X-SSI, *x* axis strength-strain index; Y-SSI, *y* axis strength-strain index; Polar-SSI, polar strength-strain index.

	PBS	PTH	OYC1	PTH + OYC1
Cortical area	0.665 ± 0.016 mm^2	0.752 ± 0.028 mm^{2a}	0.700 ± 0.040 mm^{2b}	0.778 ± 0.021 mm^{2a}
Cortical thickness	0.314 ± 0.012 mm	0.326 ± 0.007 mm	0.322 ± 0.004 mm	0.335 ± 0.013 mm [a]
PERI	4.707 ± 0.138 mm	4.827 ± 0.109 mm	4.800 ± 0.113 mm	4.800 ± 0.113 mm
ENDO	3.027 ± 0.060 mm	2.987 ± 0.180 mm	3.107 ± 0.106 mm	3.000 ± 0.166 mm
X-SSI	0.173 ± 0.011 mm^3	0.189 ± 0.010 mm^3	0.181 ± 0.016 mm^3	0.197 ± 0.014 mm^{3b}
Y-SSI	0.214 ± 0.018 mm^3	0.238 ± 0.021 mm^{3b}	0.220 ± 0.013 mm^3	0.246 ± 0.011 mm^{3a}
Polar-SSI	0.315 ± 0.021 mm^3	0.355 ± 0.024 mm^{3b}	0.332 ± 0.025 mm^3	0.367 ± 0.020 mm^{3a}

[a] $p < 0.01$ *versus* PBS (ANOVA).
[b] $p < 0.05$ *versus* PBS (ANOVA).

TABLE 2

Effects of PTH, OYC1, and PTH + OYC1 on trabecular bone indices in treated mice

	PBS	PTH	OYC1	PTH + OYC1
BV/TV	7.14 ± 1.45%	17.97 ± 6.51%[a]	15.11 ± 2.08%[a]	23.68 ± 1.78%[a]
Tb.Th	25.4 ± 2.62 μm	34.17 ± 2.06 μm[a]	32.82 ± 1.71 μm[a]	44.08 ± 2.41 μm[a,b]
N.Oc/BS	3.42 ± 0.39 1/mm	3.47 ± 1.48 1/mm	0.05 ± 0.07 1/mm[a]	0.00 ± 0.00[a]
N.Ob/BS	30.11 ± 8.95 1/mm	63.09 ± 4.32 1/mm[a]	11.13 ± 3.43 1/mm[a]	22.07 ± 3.27 1/mm[c,d]
Oc.S/BS	10.69 ± 2.45%	9.24 ± 3.61%	0.07 ± 0.11%[a]	0.00 ± 0.00%[a]
Ob.S/BS	37.41 ± 9.04%	53.75 ± 5.28%[a]	12.81 ± 3.44%[a]	26.67 ± 3.67%[a,b]
ES/BS	37.41 ± 4.50%	28.93 ± 5.27%[a]	0.18 ± 0.22%[a]	0.21 ± 0.33%[a]
MAR	3.23 ± 0.14 μm/day	5.79 ± 0.33 μm/day[a]	1.38 ± 0.19 μm/day[a]	2.14 ± 0.11 μm/day[a,b]
BFR/BS	0.53 ± 0.04 mm^3/mm^2/year	0.98 ± 0.13 mm^3/mm^2/year[a]	0.08 ± 0.02 mm^3/mm^2/year[a]	0.41 ± 0.03 mm^3/mm^2/year[a,b]

[a] $p < 0.01$ *versus* PBS (ANOVA).
[b] $p < 0.01$ *versus* OYC1 (ANOVA).
[c] $p < 0.05$ *versus* PBS (ANOVA).
[d] $p < 0.05$ *versus* OYC1 (ANOVA).

of specific RANKL inhibition on bone metastasis by cancer cells, because many cancer cells are TRAIL-sensitive. In previous studies, OPG may have partly prevented bone metastasis by inhibition of TRAIL activity, even if RANKL was the major target of OPG (21, 22).

Second, OYC1 treatment markedly reduced bone turnover. In histomorphometric analysis of femurs in OYC1-treated mice, we observed marked decreases in Oc.S/BS, N.Oc/BS, and ES/BS, indicating reduced osteoclast activities. Marked decreases in Ob.S/BS, MAR, and BFR were also observed in these mice, indicating reduced osteoblast activities. Although OYC1 inhibited both activities, osteoblasts seemed to play a dominant role in the skeletal phenotype of increased bone mass in the OYC1-treated mice. These results are consistent with previous reports showing that denosumab reduced bone turnover in huRANKL mice (24, 27). The reduction of osteoblast activities in OYC1-treated mice suggests that OYC1 suppresses coupling between bone resorption and formation by inhibiting osteoclast activities, because OYC1 did not directly affect osteoblasts (data not shown).

Third, a single subcutaneous injection of 5 mg/kg OYC1 was sufficient to increase bone mass. OYC1 had no effect at doses <1.5 mg/kg, whereas the highest dose tested (15 mg/kg) gave the best results in all tests, especially in micro-CT images. However, most of the data at 15 mg/kg OYC1 were comparable with those at 5 mg/kg. The serum OYC1 concentration 2 weeks after injection of 15 mg/kg OYC1 was twice as high as that after injection of 5 mg/kg, but the sustained OYC1 concentration (~50 μg/ml) at 5 mg/kg was high enough to increase bone mass. The serum ALP level in mice treated with 15 mg/kg OYC1 was almost half that in controls. The measured ALP activity reflects ALP from bone, placenta, intestine, kidney, and liver. The reduced ALP was probably mainly derived from bone, because RANKL functions in placenta, intestine, kidney, and liver are unknown. The reduction of the ALP level accompanied with that of TRAP-5b in OYC1-treated mice indicated coupling between bone resorption and formation.

Fourth, a single injection of 5 mg/kg OYC1 exhibited rapid and long lasting (from days 2 to 28) effects on bone mass. Bone mass increased for 4 weeks after injection of OYC1. Surprisingly, the serum OYC1 concentration 4 weeks after the injection was about 10 μg/ml. Consistent with a previous report (24), maintenance of the OYC1 concentration over 10 μg/ml was required for efficient neutralization of RANKL *in vivo*. The marked decreases of serum TRAP-5b and ALP from days 4 to 28 also demonstrated that the effect of OYC1 lasted for up to 28 days. The pharmacokinetics of 5 mg/kg OPG were similar to those of OYC1 *in vivo*, but OPG was unable to suppress Oc.S/BS, even at a serum concentration of OPG at 30 μg/ml 10 days after injection (19). Results in clinical tests show a long circulating half-life of denosumab (31). Therefore, OYC1 may be a good surrogate for denosumab for impairment of RANKL activities in normal mice. Most experiments were carried out with 6-week-old young growing mice. When 16-week-old mice were injected once with 5 mg/kg OYC1, the antibody was detected in serum 2 weeks after the injection but undetected 4 weeks after the injection (data not shown). The effect of OYC1 on the increase in BMD was significant but weak (data not shown). It may be necessary to inject OYC1 once per week or so when aged mice were used.

In short term experiments, an increase in total BMD in OYC1-treated mice was evident on day 2, and BMD and bone mass increased up to day 4. A marked reduction in the serum TRAP-5b level was observed on day 1 in OYC1-treated mice, with a 1-day delay in the decrease of serum ALP after the TRAP-5b decrease. These observations suggest that a rapid

inhibitory effect of OYC1 on osteoclasts resulted in reduction of osteoblast activities. It was notable that it took 1 day to control the coupling, with a reduction in bone formation occurring after that in bone resorption. Therefore, osteoclasts may play an important role in the coupling. There were few osteoclasts in the OYC1-treated mice on days 4, 14, and 18, and the marked decrease in serum TRAP-5b level was maintained from day 1 to day 28, indicating that the OYC1-treated mouse is a good model of osteoclast depletion.

To make use of the osteoclast-depletion model, we investigated the mechanism of the bone anabolic effect of PTH. The observation that PTH increased BMD in trabecular and cortical bone in OYC1-treated mice with few osteoclasts suggests that PTH does not require osteoclasts to exert its bone anabolic effect. In addition, OYC1 and PTH increased femoral BMD in trabecular bone independently and synergistically, indicating possible coordination of inhibition of osteoclast activities and stimulation of osteoblast activities in the treated mice. Furthermore, PTH exerted an anabolic effect on cortical bone in OYC1-treated mice, indicating that OYC1 did not blunt the bone anabolic activity of PTH. The significant increases in Tb.Th, BFR/BS, MAR, N.Ob/BS, and Ob.S/BS by administration of PTH in OYC1-treated mice with few osteoclasts strongly suggested that PTH increased bone mass by stimulating bone formation without affecting osteoclasts. The morphological changes in osteoblasts and osteocytes with PTH in OYC1-treated mice also confirmed PTH activated both cell types without affecting osteoclasts. Although PTH failed to increase serum ALP level, it showed a strong tendency to augment serum osteocalcin level in the osteoclast-depleted mice. In our experiences, administration of PTH to mice did not increase serum ALP levels. Therefore, ALP may not be a good marker of activated mouse osteoblasts with PTH.

A study by Pierroz *et al.* (27) of the effect of combination of PTH and denosumab in ovariectomized huRANKL mice showed no anabolic effect of PTH on bone mass in the lumbar spine, femoral shaft BMD, vertebral and distal femur BV/TVs, and vertebral and distal femur cortical widths in denosumab-treated mice. The different results obtained in this study may be due to differences in the experimental conditions (huRANKL mice *versus* normal mice), operation (ovariectomized *versus* no treatment), antibodies (anti-human *versus* anti-mouse), doses (10 *versus* 5 mg/kg), and period (4 weeks *versus* 4 days in pretreatment and 4 weeks *versus* 2 weeks in simultaneous treatment with PTH). In addition, huRANKL mice exhibit abnormalities such as a reduced osteoclast number and osteoblast surface compared with normal mice. We also note that Kostenuik *et al.* (32) observed an additive effects of OPG and PTH on bone density and bone strength.

We observed very few osteoclasts in mice treated with OYC1 for 4 days before PTH treatment. The decrease in the serum TRAP-5b level in mice treated with PTH and OYC1 indicated that PTH increases bone mass without activation of osteoclastogenesis in OYC1-treated mice, although PTH did activate osteoclastogenesis in normal mice. The OYC1 osteoclast-depletion mouse model was useful for investigation of the bone anabolic mechanism of PTH. The synergistic effect of OYC1 and PTH on the increase in bone mass suggests a potential use of a combination of denosumab and PTH in treatment of severe osteoporosis in humans.

REFERENCES

1. Yasuda, H., Shima, N., Nakagawa, N., Yamaguchi, K., Kinosaki, M., Mochizuki, S., Tomoyasu, A., Yano, K., Goto, M., Murakami, A., Tsuda, E., Morinaga, T., Higashio, K., Udagawa, N., Takahashi, N., and Suda, T. (1998) *Proc. Natl. Acad. Sci. U.S.A.* **95,** 3597–3602
2. Lacey, D. L., Timms, E., Tan, H. L., Kelley, M. J., Dunstan, C. R., Burgess, T., Elliott, R., Colombero, A., Elliott, G., Scully, S., Hsu, H., Sullivan, J., Hawkins, N., Davy, E., Capparelli, C., Eli, A., Qian, Y. X., Kaufman, S., Sarosi, I., Shalhoub, V., Senaldi, G., Guo, J., Delaney, J., and Boyle, W. J. (1998) *Cell* **93,** 165–176
3. Nakagawa, N., Kinosaki, M., Yamaguchi, K., Shima, N., Yasuda, H., Yano, K., Morinaga, T., and Higashio, K. (1998) *Biochem. Biophys. Res. Commun.* **253,** 395–400
4. Hsu, H., Lacey, D. L., Dunstan, C. R., Solovyev, I., Colombero, A., Timms, E., Tan, H. L., Elliott, G., Kelley, M. J., Sarosi, I., Wang, L., Xia, X. Z., Elliott, R., Chiu, L., Black, T., Scully, S., Capparelli, C., Morony, S., Shimamoto, G., Bass, M. B., and Boyle, W. J. (1999) *Proc. Natl. Acad. Sci. U.S.A.* **96,** 3540–3545
5. Simonet, W. S., Lacey, D. L., Dunstan, C. R., Kelley, M., Chang, M. S., Lüthy, R., Nguyen, H. Q., Wooden, S., Bennett, L., Boone, T., Shimamoto, G., DeRose, M., Elliott, R., Colombero, A., Tan, H. L., Trail, G., Sullivan, J., Davy, E., Bucay, N., Renshaw-Gegg, L., Hughes, T. M., Hill, D., Pattison, W., Campbell, P., Sander, S., Van, G., Tarpley, J., Derby, P., Lee, R., and Boyle, W. J. (1997) *Cell* **89,** 309–319
6. Tsuda, E., Goto, M., Mochizuki, S., Yano, K., Kobayashi, F., Morinaga, T., and Higashio, K. (1997) *Biochem. Biophys. Res. Commun.* **234,** 137–142
7. Yasuda, H., Shima, N., Nakagawa, N., Mochizuki, S. I., Yano, K., Fujise, N., Sato, Y., Goto, M., Yamaguchi, K., Kuriyama, M., Kanno, T., Murakami, A., Tsuda, E., Morinaga, T., and Higashio, K. (1998) *Endocrinology* **139,** 1329–1337
8. Shevde, N. K., Bendixen, A. C., Dienger, K. M., and Pike, J. W. (2000) *Proc. Natl. Acad. Sci. U.S.A.* **97,** 7829–7934
9. Eghbali-Fatourechi, G., Khosla, S., Sanyal, A., Boyle, W. J., Lacey, D. L., and Riggs, B. L. (2003) *J. Clin. Invest.* **111,** 1221–1230
10. Tanaka, S., Nakamura, K., Takahasi, N., and Suda, T. (2005) *Immunol. Rev.* **208,** 30–49
11. Wong, B. R., Rho, J., Arron, J., Robinson, E., Orlinick, J., Chao, M., Kalachikov, S., Cayani, E., Bartlett, F. S., 3rd, Frankel, W. N., Lee, S. Y., and Choi, Y. (1997) *J. Biol. Chem.* **272,** 25190–25194
12. Anderson, D. M., Maraskovsky, E., Billingsley, W. L., Dougall, W. C., Tometsko, M. E., Roux, E. R., Teepe, M. C., DuBose, R. F., Cosman, D., and Galibert, L. (1997) *Nature* **390,** 175–179
13. Kong, Y. Y., Yoshida, H., Sarosi, I., Tan, H. L., Timms, E., Capparelli, C., Morony, S., Oliveira-dos-Santos, A. J., Van, G., Itie, A., Khoo, W., Wakeham, A., Dunstan, C. R., Lacey, D. L., Mak, T. W., Boyle, W. J., and Penninger, J. M. (1999) *Nature* **397,** 315–323
14. Oyajobi, B. O., Anderson, D. M., Traianedes, K., Williams, P. J., Yoneda, T., and Mundy, G. R. (2001) *Cancer Res.* **61,** 2572–2578
15. Jones, D. H., Nakashima, T., Sanchez, O. H., Kozieradzki, I., Komarova, S. V., Sarosi, I., Morony, S., Rubin, E., Sarao, R., Hojilla, C. V., Komnenovic, V., Kong, Y. Y., Schreiber, M., Dixon, S. J., Sims, S. M., Khokha, R., Wada, T., and Penninger, J. M. (2006) *Nature* **440,** 692–696
16. Akiyama, T., Shimo, Y., Yanai, H., Qin, J., Ohshima, D., Maruyama, Y., Asaumi, Y., Kitazawa, J., Takayanagi, H., Penninger, J. M., Matsumoto, M., Nitta, T., Takahama, Y., and Inoue, J. (2008) *Immunity* **29,** 423–437
17. Asselin-Labat, M. L., Vaillant, F., Sheridan, J. M., Pal, B., Wu, D., Simpson, E. R., Yasuda, H., Smyth, G. K., Martin, T. J., Lindeman, G. J., and Visvader, J. E. (2010) *Nature* **465,** 798–802
18. Dougall, W. C., Glaccum, M., Charrier, K., Rohrbach, K., Brasel, K., De Smedt, T., Daro, E., Smith, J., Tometsko, M. E., Maliszewski, C. R., Armstrong, A., Shen, V., Bain, S., Cosman, D., Anderson, D., Morrissey, P. J., Peschon, J. J., and Schuh, J. (1999) *Genes Dev.* **13,** 2412–2424
19. Capparelli, C., Morony, S., Warmington, K., Adamu, S., Lacey, D., Dunstan, C. R., Stouch, B., Martin, S., and Kostenuik, P. J. (2003) *J. Bone Miner.*

Res. **18,** 852–858
20. Ominsky, M. S., Kostenuik, P. J., Cranmer, P., Smith, S. Y., and Atkinson, J. E. (2007) *Osteoporos. Int.* **18,** 1073–1082
21. Emery, J. G., McDonnell, P., Burke, M. B., Deen, K. C., Lyn, S., Silverman, C., Dul, E., Appelbaum, E. R., Eichman, C., DiPrinzio, R., Dodds, R. A., James, I. E., Rosenberg, M., Lee, J. C., and Young, P. R. (1998) *J. Biol. Chem.* **273,** 14363–14367
22. Truneh, A., Sharma, S., Silverman, C., Khandekar, S., Reddy, M. P., Deen, K. C., McLaughlin, M. M., Srinivasula, S. M., Livi, G. P., Marshall, L. A., Alnemri, E. S., Williams, W. V., and Doyle, M. L. (2000) *J. Biol. Chem.* **275,** 23319–23325
23. Yasuda, H., Shima, N., Nakagawa, N., Yamaguchi, K., Kinosaki, M., Goto, M., Mochizuki, S. I., Tsuda, E., Morinaga, T., Udagawa, N., Takahashi, N., Suda, T., and Higashio, K. (1999) *Bone* **25,** 109–113
24. Kostenuik, P. J., Nguyen, H. Q., McCabe, J., Warmington, K. S., Kurahara, C., Sun, N., Chen, C., Li, L., Cattley, R. C., Van, G., Scully, S., Elliott, R., Grisanti, M., Morony, S., Tan, H. L., Asuncion, F., Li, X., Ominsky, M. S., Stolina, M., Dwyer, D., Dougall, W. C., Hawkins, N., Boyle, W. J., Simonet, W. S., and Sullivan, J. K. (2009) *J. Bone Miner. Res.* **24,** 182–195
25. Gerstenfeld, L. C., Sacks, D. J., Pelis, M., Mason, Z. D., Graves, D. T., Barrero, M., Ominsky, M. S., Kostenuik, P. J., Morgan, E. F., and Einhorn, T. A. (2009) *J. Bone Miner. Res.* **24,** 196–208
26. Hofbauer, L. C., Zeitz, U., Schoppet, M., Skalicky, M., Schüler, C., Stolina, M., Kostenuik, P. J., and Erben, R. G. (2009) *Arthritis Rheum.* **60,** 1427–1437
27. Pierroz, D. D., Bonnet, N., Baldock, P. A., Ominsky, M. S., Stolina, M., Kostenuik, P. J., and Ferrari, S. L. (2010) *J. Biol. Chem.* **285,** 28164–28173
28. Koh, A. J., Demiralp, B., Neiva, K. G., Hooten, J., Nohutcu, R. M., Shim, H., Datta, N. S., Taichman, R. S., and McCauley, L. K. (2005) *Endocrinology* **146,** 4584–4596
29. Kamijo, S., Nakajima, A., Ikeda, K., Aoki, K., Ohya, K., Akiba, H., Yagita, H., and Okumura, K. (2006) *Biochem. Biophys. Res. Commun.* **347,** 124–132
30. Parfitt, A. M., Drezner, M. K., Glorieux, F. H., Kanis, J. A., Malluche, H., Meunier, P. J., Ott, S. M., and Recker, R. R. (1987) *J. Bone Miner. Res.* **2,** 595–610
31. Bekker, P. J., Holloway, D. L., Rasmussen, A. S., Murphy, R., Martin, S. W., Leese, P. T., Holmes, G. B., Dunstan, C. R., and DePaoli, A. M. (2004) *J. Bone Miner. Res.* **19,** 1059–1066
32. Kostenuik, P. J., Capparelli, C., Morony, S., Adamu, S., Shimamoto, G., Shen, V., Lacey, D. L., and Dunstan, C. R. (2001) *Endocrinology* **142,** 4295–4304